

# Exploring breathing pattern irregularity with projection-based method

Dan Ruan<sup>a)</sup> and Jeffrey A. Fessler<sup>b)</sup>

*Department of Electrical Engineering and Computer Science, University of Michigan, Ann Arbor, Michigan 48109*

James M. Balter<sup>c)</sup>

*Department of Radiation Oncology, University of Michigan, Ann Arbor, Michigan 48109*

Jan-Jakob Sonke<sup>d)</sup>

*The Netherlands Cancer Institute/Antoni van Leeuwenhoek Hospital, Amsterdam, The Netherlands*

(Received 3 January 2006; revised 23 March 2006; accepted for publication 27 April 2006; published 21 June 2006)

Accurate descriptions of organ motion due to breathing are highly desirable for radiation treatment planning. This paper proposes an index that quantifies the irregularity of a signal related to respiratory motion. The method works by finding the periodic band-limited signal that best fits the signal samples, and then computing the root mean squared (RMS) residual error. The fitted signal itself may be useful for treatment planning. Using clinical data describing amplitude-time relationships (RPM, Varian) from twelve patients, we correlated the proposed index against relevant metrics from various treatment planning schemes. Simulation results demonstrate a reasonable match with all treatment methods considered, suggesting that the proposed irregularity index is suitable for a variety of treatment methods. Compared to the modified cosine function, which was investigated previously for breathing pattern models, the proposed approach is more representative, flexible, and computationally efficient. © 2006 American Association of Physicists in Medicine. [DOI: 10.1118/1.2207253]

Key words: breathing irregularity index, projection

## I. INTRODUCTION

Characterization of organ motion is important in radiation therapy, including dose planning and treatment delivery.<sup>1-5</sup> Tumor motion, especially in lung/liver regions, is highly correlated with breathing patterns. Therefore, an index that characterizes breathing regularity can facilitate treatment planning for tumors in those regions, particularly for individualized treatment planning.

Periodicity has been a major assumption in breathing trajectory analysis, as good reproducibility indicates the potential for a simple structured treatment plan tailored toward the fundamental breathing pattern. Harmonic analysis has been employed widely to characterize respiratory patterns.<sup>6-8</sup> Peaks of the Fourier spectrum are often used to determine the dominating periodic behavior of the temporal trajectory. Such approaches lack a “goodness” measure, i.e., it is not clear how a periodic signal having the dominant frequency differs from the true trajectory. Consequently, no fundamental periodic pattern is available to judge the soundness of such a result.

In this paper, we propose a rigorous general framework for periodicity analysis based on subspace projections. For each period within a physiologically reasonable range, a measured breathing signal is projected onto the subspace of all signals having that period to obtain the “best fit” periodic signal in the least squared error (LSE) sense. Residual errors for each such period are then compared to yield the overall best periodic approximation. The estimated trajectory obtained by this “projection” method is therefore the closest

periodic signal with respect to observed data. We derived the method in continuous signal space to account for the sampling effect explicitly. We also allow temporal samples to be nonuniformly spaced to offer more freedom for the data acquisition procedure.

## II. METHODS AND MATERIAL

### A. Experimental setup

We used the Real-Time Position Management (RPM, Varian Medical Systems, Palo Alto, CA) system to obtain the trajectory of an external fiducial placed on each patient’s chest wall. This fiducial tracking system records data in time-displacement pairs that are generally assumed to be highly correlated with superior-inferior diaphragm motion.<sup>9</sup> This system is most useful for treating patients with tumors in the chest or lung area without compromising their breathing.

Twelve such clinical breathing signals were used in this study. The characteristic parameters of this population of data are listed in Table I.

### B. Technical problem formulation

Given a set of discrete samples of a breathing trajectory, we want to find the periodic signal that best matches the observation data. This is equivalent to reconstructing a periodic signal of unknown period from its noisy discrete samples. For this problem to be feasible, we assume that there is some maximal frequency component in the signal. This assumption is physiologically reasonable. We thus focus

TABLE I. Data set information and experiment results.

ID V.S. Parameter	1	2	3	4	5	6	7	8	9	10	11	12
	Data characterization <sup>a</sup>											
STD (cm)	0.158	0.210	0.266	0.242	0.206	0.259	0.242	0.267	0.283	0.313	0.335	0.202
	Breathing trajectory fitting with modified cosine model											
period (s)	4.7	4.6	4.9	5.3	5.3	4.3	4.9	6.4	9.5	5.6	3.0	5.3
RMSE (cm)	0.138	0.171	0.216	0.139	0.193	0.224	0.145	0.208	0.153	0.096	0.337	0.169
Dose error (%)	1.667	2.793	3.527	2.092	3.217	3.580	2.402	3.293	2.496	1.454	6.144	2.161
PTV margin (cm)	5.940	5.900	5.523	5.723	5.727	5.859	5.646	5.338	5.724	5.522	5.951	5.835
95% dose coverage	0.909	0.887	0.850	0.904	0.878	0.851	0.906	0.858	0.890	0.938	0.811	0.888
	Breathing trajectory fitting with projection method											
Period (s)	4.7	4.4	4.5	5.4	4.1	4.6	4.7	7.2	9.7	5.6	3.1	5.2
RMSE (cm)	0.135	0.155	0.102	0.132	0.162	0.127	0.115	0.075	0.148	0.090	0.328	0.166
Dose error (%)	1.595	2.440	1.638	1.983	2.352	1.721	1.832	1.210	2.471	1.431	6.137	2.066
95% dose coverage	0.915	0.903	0.934	0.903	0.876	0.910	0.924	0.949	0.905	0.942	0.836	0.895
	Result for 20 s training, 10 s testing											
Period (s) <sup>b</sup>	4.2	4.2	4.5	5.2	4.3	4.8	4.8	7.3	9.0	5.7	3.0	5.0
RMSE <sub>train</sub> (cm) <sup>c</sup>	0.153	0.151	0.089	0.126	0.082	0.075	0.121	0.042	0.116	0.078	0.228	0.049
RMSE <sub>test</sub> (cm) <sup>d</sup>	0.177	0.256	0.150	0.231	0.318	0.283	0.141	0.147	0.290	0.150	0.580	0.3062

<sup>a</sup>Data are normalized to have zero mean and 1 cm peak to peak variation.

<sup>b</sup>This period is obtained from the training data (first 20 s the breathing trace only).

<sup>c</sup>RMSE evaluated with the training data only.

<sup>d</sup>RMSE evaluated by extending the periodic pattern obtained from training to the test portion of the breathing trace.

on the subspace of band-limited periodic signals. We formulate the problem in a multilayer optimization setup where we search over all possible periods for the “best-fit” signal. For each period within a reasonable range, the observed breathing trajectory is projected onto the subspace of all band-limited signals having that period to obtain the closest matching periodic function. Projections from each such subspace are then compared to yield the overall best periodic approximation. This method accounts for the discrete temporal sampling explicitly, and allows for the possibility of non-uniform sampling.

We model the observation data  $y_i$  as a temporal trajectory sampled at  $\{t_i\}_{i=1}^N$  with additive noise:

$$y_i = f(t_i) + n_i, \quad i = 1, 2, \dots, N, \quad (2.1)$$

where  $f$  is the unknown ground-truth continuous periodic function whose spectrum has finite support between  $[-\gamma, \gamma]$  and  $n_i$  denotes the additive noise.

If  $f(t)$  is a band-limited function with period  $T$ , then we follow Ref. 10 to rewrite it as linear combination of Fourier harmonics:

$$f(t) = \sum_{k=-K}^K c_k e^{j2\pi kt/T}, \quad K = \left\lfloor \frac{T}{2\Delta t} \right\rfloor, \quad (2.2)$$

where  $c_k$ 's are the coefficients for Fourier harmonics,  $\Delta t \triangleq \min_i(t_i - t_{i-1})$ , and  $\lfloor \cdot \rfloor$  denotes the floor function.

Evaluation of the above representation at  $\{t_i\}_{i=1}^N$  can be compactly rewritten in vector form as

$$\mathbf{f} = \mathbf{G}_T \mathbf{c}, \quad (2.3)$$

where  $\mathbf{f} = [f(t_1), f(t_2), \dots, f(t_N)]^T$  denotes the discrete samples of the underlying function  $f$ ;  $\mathbf{c} = [c_{-K}, c_{-K+1}, \dots, c_K]^T$  is the concatenation of Fourier coefficients; and the matrix  $\mathbf{G}$  is defined as

$$\mathbf{G}_T(i, k) = e^{j2\pi kt_i/T}. \quad (2.4)$$

Therefore, given the observed sample trajectory  $\mathbf{y} = [y_1, y_2, \dots, y_N]^T$ , the optimal period  $T^*$  is the solution to the following optimization problem:

$$T^* = \underset{T}{\operatorname{argmin}} \min_{\mathbf{c} \in \mathbb{C}^{2K+1}} \|\mathbf{y} - \mathbf{G}_T \mathbf{c}\|^2, \quad (2.5)$$

where  $\mathbb{C}^{2K+1}$  is the set of vectors of length  $(2k+1)$ , and  $\|\mathbf{y}\|^2 = \sum_{i=1}^N |y_i|^2$ . The closest periodic signal to the sampled trajectory in LSE sense is then given by

$$f^*(t) = \sum_{k=-K}^K \hat{c}_k e^{j2\pi kt/T^*}, \quad (2.6)$$

where  $K = \lfloor T^*/2\Delta t \rfloor$  and  $\hat{c}_k$  are obtained as the components of solution to Eq. (2.7) when  $T = T^*$ .

For a given candidate period  $T$ , the bandwidth parameter  $K = \lfloor T/2\Delta t \rfloor$  is a constant, and the inner optimization problem becomes an ordinary least-squares minimization:

$$\mathbf{c}_T^* = \underset{\mathbf{c} \in \mathbb{C}^{2K+1}}{\operatorname{argmin}} \|\mathbf{y} - \mathbf{G}_T \mathbf{c}\|^2. \quad (2.7)$$

From classical optimization theory,<sup>11</sup> the optimal  $\mathbf{c}_T^*$  of Eq. (2.7) satisfies the normal equation:

$$(\mathbf{G}_T^* \mathbf{G}_T) \mathbf{y} = \mathbf{G}_T^* \mathbf{c}_T^* \quad (2.8)$$

where  $\mathbf{G}_T^*$  is the conjugate transpose of  $\mathbf{G}_T$  and  $\mathbf{G}_T^* \mathbf{G}_T$  is known as the Gram matrix.

Moreover, when the sample size is large enough, specifically  $N \geq 2K + 1$ , which we assume hereafter,  $\mathbf{G}_T$  has full column rank, and the  $(2k + 1) \times (2k + 1)$  Gram matrix  $\mathbf{G}_T^* \mathbf{G}_T$  is invertible.<sup>12</sup> The optimal solution for Eq. (2.8) can be written explicitly as

$$\mathbf{c}_T^* = (\mathbf{G}_T^* \mathbf{G}_T)^{-1} \mathbf{G}_T^* \mathbf{y}. \quad (2.9)$$

At this point, we have solved the inner optimization problem in Eq. (2.5) in closed form. The feasible range of periods  $T$  in the outer minimization can be designed by incorporating physical knowledge. For instance, normal breathing is expected to have a period between 1 and 10 s. Moreover, even though the peak of the Fourier spectrum is not informative enough by itself, it turns out to be a reasonably good initialization for our method. Notice that if exhaustive search over  $T$  is to be applied in 2.5, we need to evaluate Eqs. (2.9) and (2.6) for each  $T$  of interest. Thus the computation cost depends both on how finely we sample the period parameter  $T$  and the range of search. Using a good initial guess for  $T^*$  can reduce the search range and thus reduce computation substantially. Also, reasonable initialization helps to prevent the algorithm from falling into nonphysical local minima. Since it is now a simple one-dimensional optimization problem to find  $T^*$ , we use an exhaustive line search over a relatively small interval thanks to a good Fourier-based initialization. Alternative optimization approaches like multiresolution or incremental refinement could be used to speed up the process. Due to the use of superposition of harmonics to describe periodic functions, projection to the subspace corresponding to periodic functions with period  $2T$  would naturally yield a better data fit than the projection onto the subspace for period  $T$ . In other words, a function of period  $T$  is certainly a function of period  $2T$ , but not vice versa. However, the additional descriptive power may not always be desirable, since this could cause overfitting introduced by noise. Initialization by detecting the peak of the Fourier spectrum picks out the dominant harmonic component and the algorithm only needs to search over a relatively small neighborhood around that initialization point, with the confidence that the local minimal obtained would be physiologically optimal.

Finally, our proposed irregularity index is the root mean squared error (RMSE) between the overall optimal periodic signal and the measured trajectory:

$$\text{RMSE} = \sqrt{\frac{1}{N} \sum_{i=1}^N \|f^*(t_i) - y_i\|^2}. \quad (2.10)$$

### C. Verification and test design

Under Institutional Review Board (IRB) approved protocol, we have used the RPM system (Varian, Palo Alto, CA) to obtain breathing trace data recorded at 10 Hz with duration 30 s from 12 different patients. The recorded RPM data

have relative units. To better illustrate the major idea in this paper, we normalize all the breathing trace data to have uniform zero mean and 1 cm peak-to-peak variation. Shifting the mean does not introduce any bias into any treatment simulation since it is a global quantity; while normalizing the amplitudes makes the data more representative of typical tumor motion induced by respiratory motion. The standard deviations of these normalized data are listed in Table I. To justify the soundness of the proposed irregularity index, we have virtually simulated a one-dimensional phantom object of size 5 cm that moves according to the observed trajectories to mimic the behavior of a 5 cm size tumor with peak-to-peak motion about 1 cm, which is realistic in clinical situations. A single ideal one-dimensional treatment beam, or in fact, delivery pattern of the same size (5 cm) is designed for dose delivery simulations. It has no penumbra, and completely covers the simulated target with uniform radiation intensity. This idealized energy deposition model will be used hereafter to illustrate the potential impact of motion patterns and how they influence energy deposition.

To verify that the proposed “irregularity index” and the fundamental pattern obtained from the projection model are clinically significant, we have designed three sets of experiments.

First, we show that the RMSE, which is a mathematical criterion, is well correlated with clinically critical metrics. In this paper, we use dose error, planning target volume (PTV) margin and 95% dose coverage to characterize performances. In particular, dose error is computed in percent as the normalized difference between received dose and the ideal dose that corresponds to a perfect overlap between the target and treatment beam throughout the whole treatment procedure; PTV margin is the expansion needed to ensure that the entire clinical target volume receives the prescribed dose; and 95% dose coverage is computed as the portion of the target that receives no less than 95% of the designated dose with no margin. To account for the interplay between target motion and treatment beam adjustment, the phantom object is moved conforming to the observed breathing trace and the treatment beam is scheduled according to a designated pattern. We evaluate both the periodic fundamental pattern extracted with the projection model in 2.6 and the one obtained with the optimal commonly used modified cosine model<sup>13,14</sup> to control the movement of the treatment plan. The modified cosine model assumes that the breathing trajectory conforms to the following formula:

$$z(t) = z_0 - a \cos^{2n}(\pi t / \tau - \phi), \quad (2.11)$$

where  $z_0, a, n, \tau, \phi$  are assumed to correspond to exhalation position, motion amplitude, asymmetry degree, period, and phase offset, respectively, and are parameters to be optimized;  $z(t)$  represents the breathing trace index by time.

Dose error, PTV margin, and 95% dose coverage are compared against RMSE in both setups to demonstrate the correlation.

Second, we compare the projection-based model with the modified cosine model (2.11) to test the feasibility of the

obtained fundamental pattern. RMSE as well as dose error, PTV margin, and 95% dose coverage are used for this comparison.

Third, we illustrate the potential clinical use of the proposed method to predict motion induced by respiration. We partitioned the breathing trace into two parts: a training part of duration 20 s and a testing part of duration 10 s. For each breathing trace, the projection model is learned with the training trajectory only, and it is used to “predict” the breathing behavior for the testing portion. This is essentially a test of temporal variance.

### III. RESULTS AND DISCUSSION

Figure 1 shows one patient data set to illustrate the role Fourier-initialization plays in avoiding suboptimal local minima. An exhaustive evaluation for RMSE was carried out over a large range of candidate periods in Fig. 1(a). Figure 1(b) illustrates the nonphysiological optimal obtained without proper prior information, for the reason we discussed previously: harmonic analysis has an inherent bias toward large period. Figure 1(c) shows that initializing with peak location of Fourier spectral (in this example corresponding to  $T=4.3$  s) helps to correctly capture the physiologically sound optimal period and enables us to restrict the period search to an even smaller candidate set for further computation efficiency.

To validate the correlation between the RMSE and the clinically critical metrics, we plot the performance characteristic parameters (dose error, PTV margin, 95% dose coverage) versus RMSE in Fig. 2 for both projection model based motion compensated treatment and modified cosine model based motion compensated treatment. Quantitative results are listed in Table I. In both treatment plan simulations, dose error and PTV margin demonstrate an increasing trend as RMSE becomes larger while the 95% dose coverage decreases. This validates the soundness of using RMSE as the index for “performance indicator.”

Moreover, we carry out a comparison between the projection-based model with the commonly used modified cosine model described in Eq. (2.11). Figure 3 shows the RMSE of the best fit modified cosine model versus the proposed index (RMSE derived from projection model), and it demonstrates that not only does our index capture how well the signal can be approximated by a well-recognized physical model, but the fundamental pattern obtained via the projection model uniformly outperforms the modified cosine model in the LSE sense. For further clinically meaningful justification, we calculate the performance characteristic parameters corresponding to a modified cosine model in Table I, and we can observe that our projection model yields lower RMSE, dose error, PTV margin, and higher dose coverage than the modified cosine model overall (Fig. 3). Furthermore, the problem of fitting the data to the model described by Eq. (2.11) is highly nonconvex with respect to its parameters which incurs two issues: it is extremely sensitive to initialization due to the numerous local minima; and it is computationally expensive as a nontrivial high dimensional search

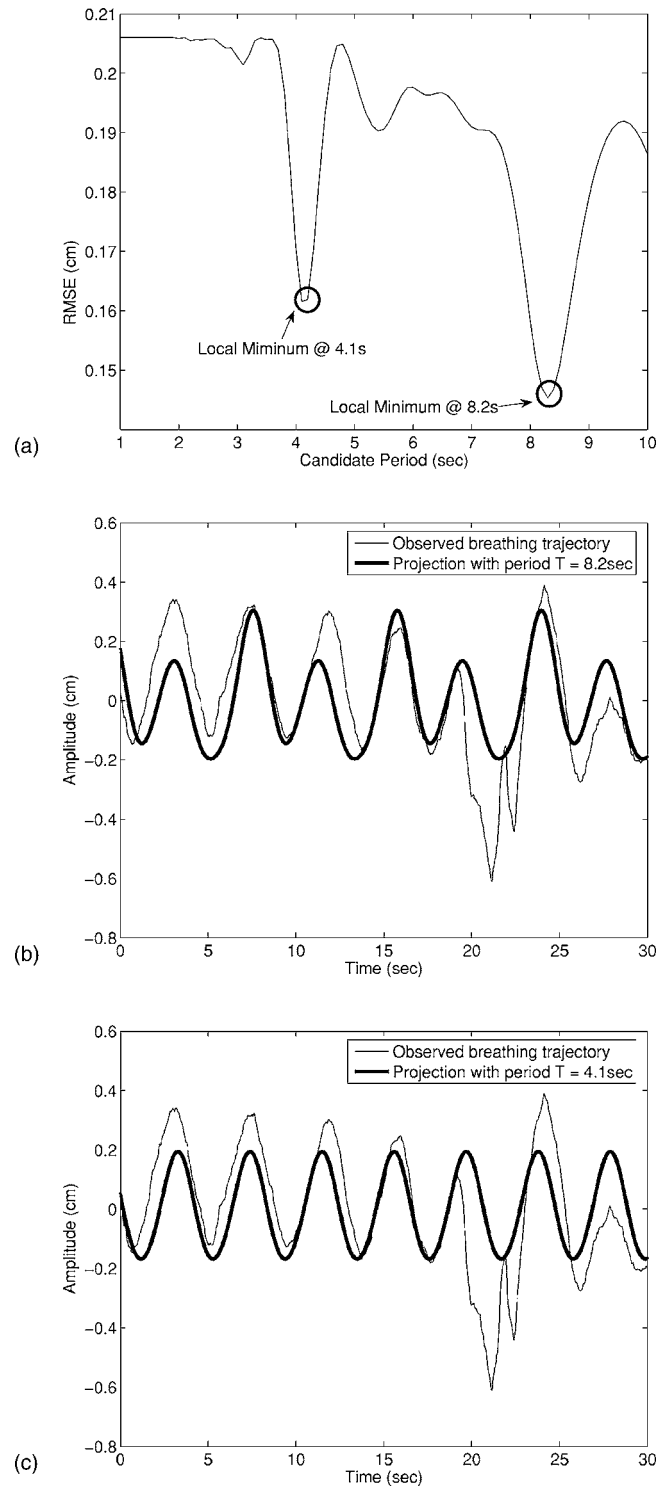


FIG. 1. Proper initialization helps to avoid suboptimal (nonphysical) local minimum: (a) Exhaustive evaluation of RMSE for difference candidate periods; (b) estimated pattern at  $T=8.2$  s, this is nonphysical even though it corresponds to slightly better fitting in RMSE sense; (c) estimated pattern at  $T=4.1$  s, the physiologically sound optimal period.

problem. In contrast, the proposed projection approach offers a closed form solution for the inner optimization problem in Eq. (2.5) and is thus simplified to a one-dimensional line search, it has an obvious advantage in computation efficiency over the modified cosine model.

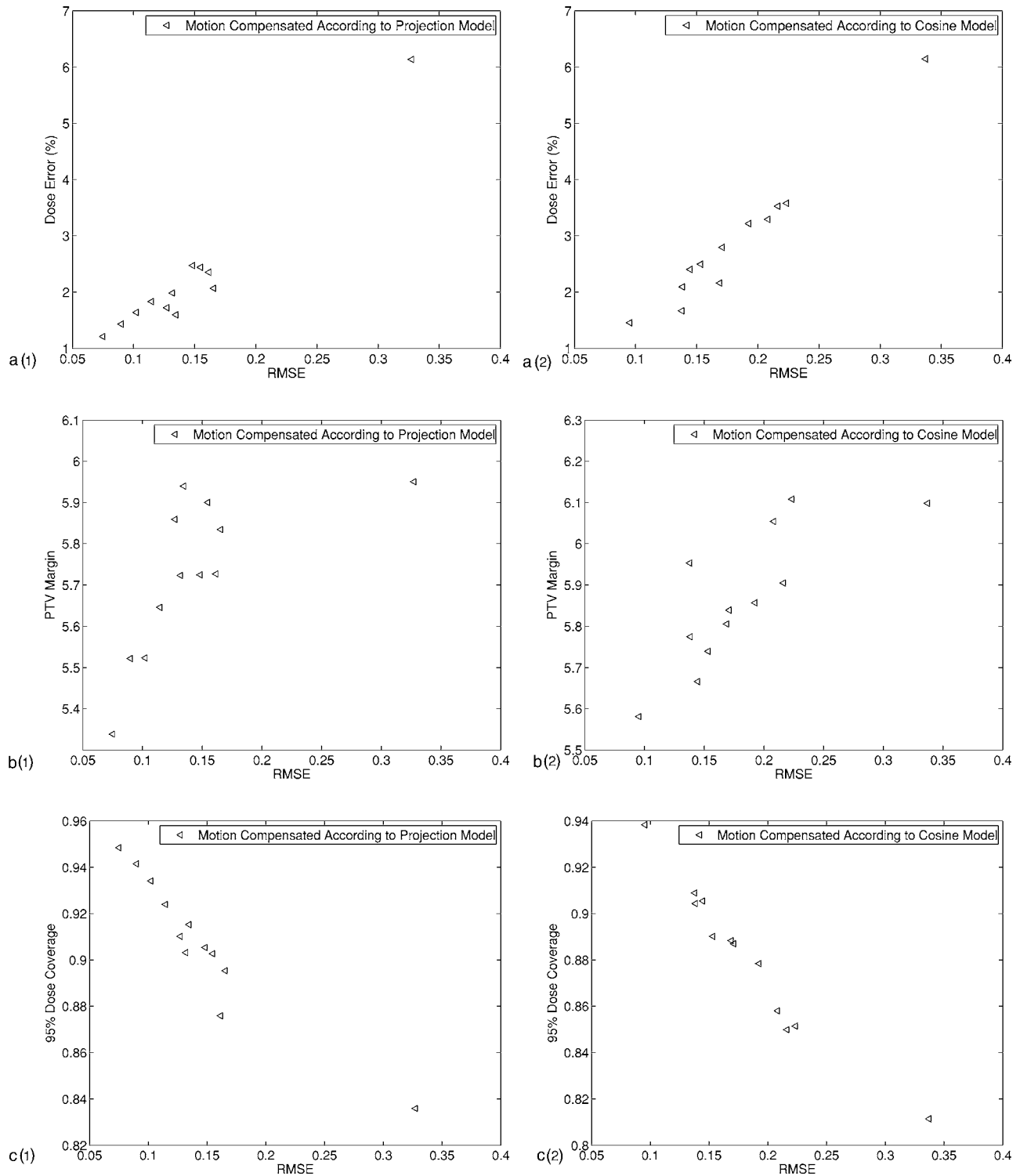


FIG. 2. Clinical significant performance metrics vs Root Mean Squared Error (RMSE). Different metrics are indicated with letters [(a#)] dose error (%); [b(#)] PTV margin (cm); [c(#)] 95% dose coverage. Different motion models for comoving the treatment beam are indicated with numbers: [X(1)] projection based model (treatment beam trajectory described as linear combinations of harmonics); [X(2)] modified cosine model.

To further justify the above-mentioned claims, Fig. 4 shows some of the fitted trajectories with “optimal” cosine model parameters with their counterparts from the projection-based approach. The fundamental patterns obtained by the projection method do indeed offer a better match than the cosine model. This is a result of the intrinsic

“nonparametric” nature of the projection based approach. Described as a linear combination of harmonics, the fundamental pattern has essentially  $(2K+1)$  degrees of freedom where  $K$  is determined by the imposed band limit of the physical signal. The modified cosine model, on the other hand, has explicitly assumed no more than 5 degrees of free-

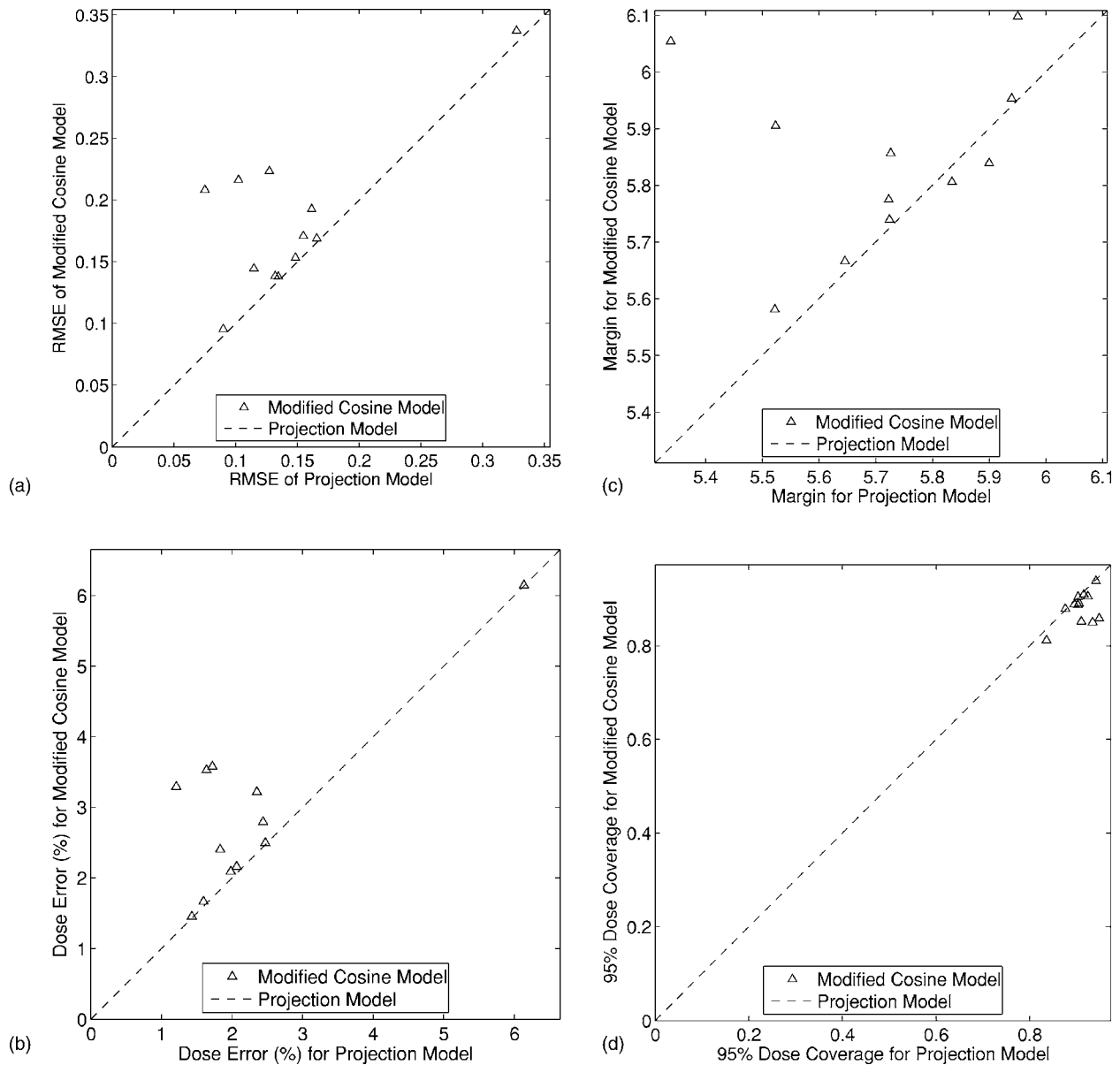


FIG. 3. RMSE, dose error (%), PTV margin (cm), 95% dose coverage of modified cosine model vs projection model.

dom, which has restricted its descriptiveness. For the same reason, our method imposes no symmetry on the fundamental pattern; in particular, the trajectory of inhalation does not have to be the inverse of exhalation, unlike the modified cosine model.

A “good” fit of the breathing trace with a periodic pattern is obtained (low RMSE by the proposed irregularity index) indicating that the breathing trace under examination is highly regular, and vice versa. Similar argument holds for the relationship between “bad” fit (high RMSE) and high irregularity. Instead of examining the combination of a whole bunch of quantities, such as standard deviation of amplitude, mean positions, periods of breathing cycles, etc., this single number (the RMSE) serves as the irregularity index, since it is designed specifically for this purpose. Therefore, observing a low RMSE increases the confidence and feasibility for potential dynamic treatment for the mobile target. In particu-

lar, synchronized moving aperture radiation therapy<sup>15</sup> and similar motion compensation based treatment schemes are potentially applicable. Moreover, the fundamental pattern, which is obtained as a free side-product during the process of estimating period and computing the irregularity index, is a good indicator of what the radiation beam pattern should be, serving the same purpose as average tumor trajectory (ATT) introduced in Ref. 15. In other words, it can be regarded as an alternative derivation of ATT without having to examine individual cycles too closely. A potential merit of the proposed method for extracting ATT is that it is much less sensitive to additive noise due to its global nature—every sample on the observed-breathing trace contributes to the estimation of the fundamental pattern.

To show the potential application of the proposed projection based scheme to predict target motion, we derive the fundamental pattern with the first 20 s of breathing trace (the

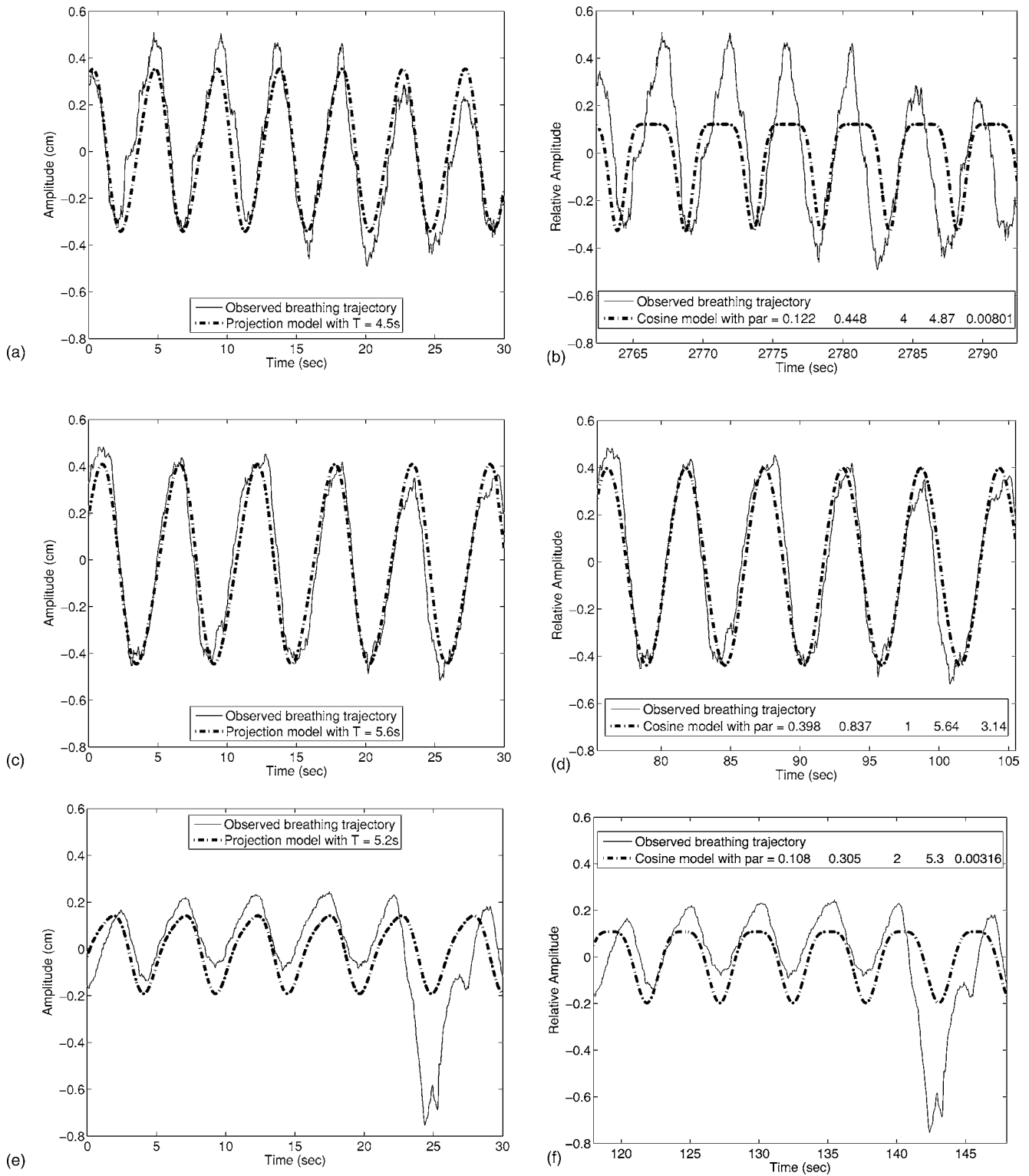


FIG. 4. Left column: projection model vs true trajectory; right column: modified cosine model vs true trajectory.

training portion) and apply it to the remainder of the data—the next 10 s of breathing trajectory is called “testing portion” since it is not seen by the projection model. We illustrate some examples in Fig. 5. The irregularity indexes derived from the learning portion, the corresponding optimal

period, and the evaluation of its fit to the ground-truth trajectory for the testing portion using RMSE are provided in Table I.

The quality of the prediction depends on how repetitive the true breathing trajectory is, which again can be measured

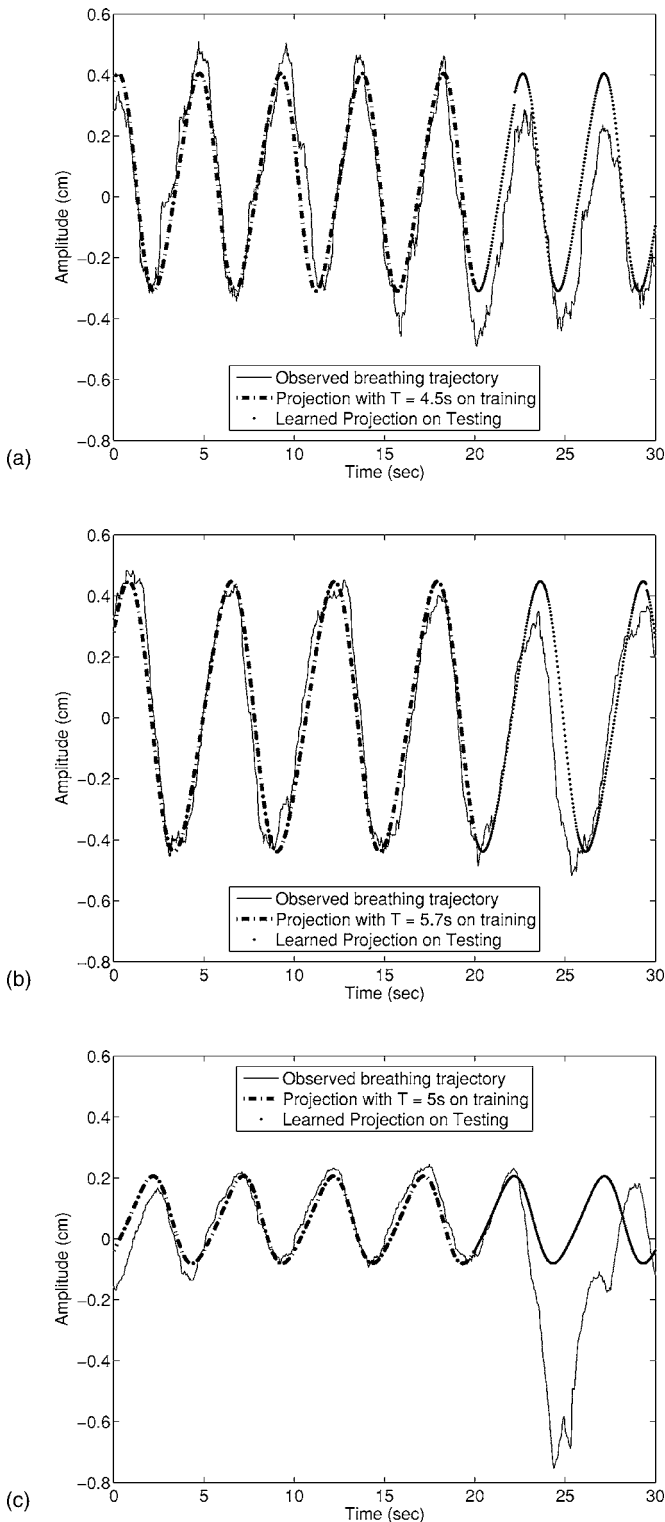


FIG. 5. Prediction of breathing trajectory with projection model.

by the proposed regularity index. When we examine closely the RMSE computed from training portion and test portion, we will see that the latter is uniformly larger, which is expected (since optimization is applied only to training data). Moreover, when we examine across cases, there is a positive correlation between RMSE computed during training and RMSE computed from testing. This indicates RMSE during

recent historical trajectory is a good predictor for RMSE, and thus irregularity level for near future. Generally, being a global regularity measure, the proposed index may not capture time varying properties of the breathing signal. This limitation can be overcome by applying the proposed method to smaller sliding time intervals instead of the whole trace.

Despite this limitation, the projection model based prediction appears to provide reasonable predictions within approximately a 2 s response window given a sufficiently regular breathing trace. Even though this number is significantly larger than the 0.4 s discussed in Ref. 9, we are *not* claiming that the proposed algorithm is preferable to adaptive filtering, since regularity in breathing trace is a pretty stringent assumption. Modeling of free form breathing is a hard and unsolved problem in general. It is often desirable to have a simple and descriptive model even if some conditions need to be checked in the first place. Moreover, the proposed irregularity index is a convenient tool for such a sanity check. By examining this single index, we can determine whether the breathing trace is regular enough for the periodicity assumption to hold, hence the corresponding prediction or synchronized motion compensation with ATT may be applied.

#### IV. CONCLUSIONS AND FUTURE WORK

We have derived a general framework to find the closest periodic signal that best matches the temporally sampled observation of breathing trajectory. Experimental results have shown good consistency with physical knowledge and clinically critical parameters as dose percentage error, PTV margin, and 95% dose volume. Comparison between the popular modified cosine breathing model and the projection-based approach shows that being consistent with the residual error from fitting the modified cosine model, our approach offers additional computation efficiency and robustness in the optimization process. Furthermore, we get the fundamental breathing pattern which helps to justify the soundness of the results and can serve as a valuable reference in further treatment planning. Potential applications of the fundamental pattern to dynamic motion compensation and prediction are illustrated with preliminary experiments. It is also likely that knowledge of the periodic signal can aid in reconstruction of four-dimensional computed tomographic models.

In this study, we have focused on finding the optimal periodic signal in the LSE sense. As future work, we would like to investigate alternative metrics that are potentially more tolerant to transient pathological breathing patterns. Also, for a particular treatment planning scheme, some choice of matching metrics could be more suitable than others, and the design of plan-dependent irregularity indexes would be interesting. Finally, we have used in this study the RMSE resulting from the projection method as an irregularity index. Potential variants, for instance, a normalized version, may be more desirable in some applications.

#### ACKNOWLEDGMENT

This work is supported in part by NIH Grant No. P01-CA59827.



- <sup>a)</sup>Electronic mail: druan@umich.edu
- <sup>b)</sup>Electronic mail: fessler@umich.edu
- <sup>c)</sup>Electronic mail: jbalter@med.umich.edu
- <sup>d)</sup>Electronic mail: j.sonke@nki.nl
- <sup>1</sup>T. Bortfeld, K. Jokivarsi, M. Goitein, J. Kung, and S. Jiang, "Effects of intra-fraction motion on imrt dose delivery: Statistical analysis and simulation," *Phys. Med. Biol.* **47**, 2203–2220 (2002).
- <sup>2</sup>C. S. Chui, E. Yorke, and L. Hong, "The effects of intra-fraction motion on the delivery of intensity-modulated field with a multileaf collimator," *Med. Phys.* **30**, 1736–1746 (2003).
- <sup>3</sup>R. George, P. Keall, V. Kini, S. Vedam, J. Siebersand, Q. Wu, M. Lauterbach, D. Arthur, and R. Mohan, "Quantifying the effect of intrafraction motion during breast imrt planning and dose delivery," *Med. Phys.* **30**, 552–562 (2003).
- <sup>4</sup>D. Gierga, G. Chen, J. Kung, M. Berke, J. Lombardi, and C. Willett, "Quantification of respiration-induced abdominal tumor motion and its impact on imrt dose distributions," *Int. J. Radiat. Oncol., Biol., Phys.* **58**, 1584–1595 (2004).
- <sup>5</sup>S. Jiang, C. Pope, K. Al. Jarrah, J. Kung, T. Bortfeld, and G. Chen, "An experimental investigation on intra-fractional organ motion effects in lung imrt treatments," *Phys. Med. Biol.* **48**, 1773–1784 (2003).
- <sup>6</sup>C. Riviere, A. Thakral, I. I. Iordachita, G. Mitroi, and D. Stoianovici, "Predicting respiratory motion for active canceling during percutaneous needle insertion," in *Proc. 23rd Annual Intl. Conf. IEEE Engineering in Medicine and Biology Society*, pp. 3477–3480, Oct. 2001.
- <sup>7</sup>R. Peslin, C. Gallina, C. Saunier, and C. Duvivier, "Fourier analysis versus multiple linear regression to analyse pressure-flow data during artificial ventilation," *Eur. Respir. J.* **7**, 2241–2251 (1994).
- <sup>8</sup>R. P. Hamalainen and A. Kettunen, "Stability of Fourier coefficients in relation to changes in respiratory air flow patterns," *Med. Eng. Phys.* **22**, 733–739 (2000).
- <sup>9</sup>S. S. Vedam, P. J. Keall, A. Docef, D. A. Todor, V. R. Kini, and R. Mohan, "Predicting respiratory motion for four-dimensional radiotherapy," *Med. Phys.* **31**, 2274–2283 (2004).
- <sup>10</sup>H. G. Feichtinger, K. Gröchenig, and T. Strohmer, "Efficient numerical methods in non-uniform sampling theory," *Numer. Math.* **69**, 423–440 (1995).
- <sup>11</sup>D. G. Luenberger, *Optimization by Vector Space Methods* (Wiley, New York, 1969).
- <sup>12</sup>K. Gröchenig, "A discrete theory of irregular sampling," *Linear Algebr. Appl.* **193**, 129–150 (1993).
- <sup>13</sup>A. E. Lujan, E. W. Larsen, J. M. Balter, and R. K. Ten Haken, "A method for incorporating organ motion due to breathing into 3d dose calculations," *Med. Phys.* **26**, 715–720 (1999).
- <sup>14</sup>A. E. Lujan, J. M. Balter, and R. K. Ten Haken, "A method for incorporating organ motion due to the breathing into 3d dose calculations in the liver: Sensitivity to variations in motion," *Med. Phys.* **30**, 2643–2649 (2003).
- <sup>15</sup>T. Neicu, H. Shirato, Y. Seppenwoolde, and S. B. Jiang, "Synchronized moving aperture radiation therapy (smart): Average tumour trajectory for lung patients," *Phys. Med. Biol.* **48**, 587–598 (2003).